Nematic cells with quasicrystalline-patterned alignment layers

Michael H. Schwarz and Robert A. Pelcovits
Department of Physics, Brown University, Providence, Rhode Island 02912, USA
(Received 6 October 2008; published 2 February 2009)

Nematic cells with surface anchoring fields exhibiting quasicrystalline symmetry can be fabricated using linear photopolymerizable polymers and suitable optics. Using the Lebwohl-Lasher model we carry out Monte Carlo simulations of a nematic cell where the top and bottom surfaces have an anchoring field with the symmetry of a periodic approximant to a Penrose lattice. We show that the anchoring field has point topological defects, nearly all with topological charge ± 1. Our simulations, which assume infinitely strong anchoring of the nematic to the anchoring field, show that half-integer disclination lines emerge from the point defects and either traverse the thickness of the cell for small cell thicknesses, hug the patterned surfaces for large thicknesses, or combine these behaviors for intermediate thicknesses. We show that estimates of the values of the thicknesses separating these three behaviors can be obtained using the properties of Penrose tilings.

DOI: 10.1103/PhysRevE.79.022701 PACS number(s): 61.30.Hn, 61.30.Jf, 61.30.Gd

Novel patterning of the director alignment surfaces that bound the top and bottom of a nematic display cell can be achieved using linear photopolymerizable polymers exposed to holographically generated polarization interference patterns [1–3]. The liquid crystal molecules near the surface can be made to align parallel or perpendicular to the local polarization direction on the surfaces of the cell. Depending on the interference pattern created, the alignment layers can exhibit either one- or two-dimensional modulation of the director anchoring field, including structures with crystalline or quasicrystalline symmetry and point topological defects.

In previous work [4] we carried out numerical simulations of the director ordering in a cell where the anchoring field exhibited fourfold symmetry, with a pattern of ± 1 point topological defects occupying interpenetrating square lattices. We showed that for thin enough samples the point defects on opposite surfaces are joined by $\pm 1/2$ disclination lines traversing the cell, whereas for thicker samples it is energetically favorable for the disclination lines to minimize their length by hugging the patterned surfaces and joining point defects on the same surface. In the latter situation the disclination lines are oriented along the diagonals of the square lattice and the direction of the cell's nematic order is along the same direction.

Here we report on numerical simulations of cells patterned with alignment layers exhibiting quasicrystalline symmetry, specifically fivefold symmetry. While the overall physical picture is similar to that considered in Ref. [4], in terms of disclination lines spanning the thickness of the cell for small cell thicknesses and hugging the surfaces for large cell thicknesses, the defect structure of the anchoring field and the orientation of the disclination lines for thick samples is more complicated than in the case of square lattice symmetry.

An anchoring field with fivefold symmetry can be created from the interference of ten laser beams, each making the same angle with an axis perpendicular to the anchoring surfaces (which we choose to be the z axis), and distributed azimuthally along the ten directions given by

$$\mathbf{e}_i = \left[\cos\left(\frac{2\pi(i-1)}{5}\right), \sin\left(\frac{2\pi(i-1)}{5}\right)\right], \quad i = 1, \ldots, 5 \tag{1}$$

and their inverted images $-\mathbf{e}_i$. For light polarized within the plane of the anchoring surfaces, the time-independent part of the electric field produced by the superposition of the ten beams is given by

$$\mathbf{E}(\mathbf{r}_\perp) = \sum_{i=1}^{5} \cos(k\mathbf{e}_i \cdot \mathbf{r}_\perp)\mathbf{e}_{i\perp}, \tag{2}$$

where

$$\mathbf{e}_{i\perp} = \hat{\mathbf{z}} \times \mathbf{e}_i = \left[-\sin\left(\frac{2\pi(i-1)}{5}\right), \cos\left(\frac{2\pi(i-1)}{5}\right)\right], \tag{3}$$

$\mathbf{r}_\perp = (x, y)$, and k is the magnitude of the projection of the beam wave vector on the anchoring surface.

This electric field has pentagrid symmetry and a pentagrid is dual to a Penrose tiling [5] (see Fig. 1). Given that

$$\nabla(\hat{\mathbf{z}} \cdot \nabla \times \mathbf{E}) = k^2 \mathbf{E}_\perp, \tag{4}$$

where $\mathbf{E}_\perp = \hat{\mathbf{z}} \times \mathbf{E}$, we see that $\mathbf{E}_\perp$ is perpendicular to curves of constant $\phi \equiv \hat{\mathbf{z}} \cdot \nabla \times \mathbf{E}$, while $\mathbf{E}$ is tangent to these curves. This provides a convenient way of visualizing the electric field (see Fig. 1), as well as information about topological defects in the anchoring field. Since $\mathbf{E}$ is tangent to curves of constant ϕ, topological defects in the anchoring field (which we assume is parallel to $\mathbf{E}$) can only occur at critical points, i.e., maxima, minima, or saddle points of ϕ, which occur when $\frac{\partial \phi}{\partial x} = 0$ and $\frac{\partial \phi}{\partial y} = 0$. In addition, the type of critical point determines the charge of the topological defect. Maxima and minima of ϕ, where the Hessian determinant of ϕ [denoted $h(\phi)$ and defined by $h(\phi) \equiv \frac{\partial^2 \phi}{\partial x^2}\frac{\partial^2 \phi}{\partial y^2} - (\frac{\partial^2 \phi}{\partial x \partial y})^2$] is positive, correspond to defects of charge $+1$, with $\mathbf{E}$ tangent to closed curves of constant ϕ encircling the defect point. Ordinary saddles of ϕ where $h(\phi)$ is negative correspond to defects of charge -1. Using numerical methods we have found that nearly all of the critical points of ϕ have nonzero Hessian determinant, and thus, nearly all of the topological defects of

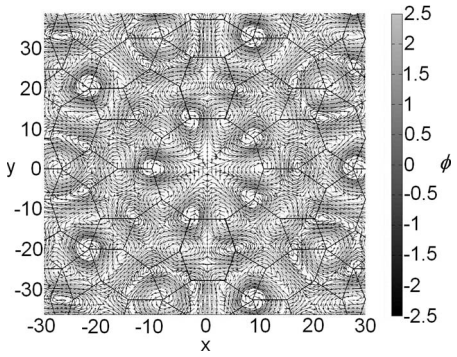

FIG. 1. Plot of curves of constant $\phi \equiv \hat{\mathbf{z}} \cdot \nabla \times \mathbf{E}$ (using the scale on the right) and the unit vector field $\mathbf{E}/E$, showing that $\mathbf{E}$ [Eq. (2)] is tangent to curves of constant ϕ. Also shown is the Penrose tiling which is dual to the pentagrid determined by the vectors $\mathbf{e}_i$, $i=1,\ldots,5$. This pentagrid has a point (0,0) where five grid lines meet, whose dual in the Penrose tiling is a decagon, and points along the grid lines through (0,0) where three grid lines meet, whose duals in the Penrose tiling are hexagons. The duals of all other points in this pentagrid are rhombi.

the anchoring field have charge ± 1. For example, we have found that for $k=1$ there are approximately 293 critical points of ϕ in the domain $-30<x<30$, $-30<y<30$, and that one of them [namely, $(x,y)=(0,0)$] has $h(\phi)=0$. At $(x,y)=(0,0)$ there is a fivefold symmetric saddle point in ϕ and a defect of charge -4 occurs. We conjecture that in general $(x,y)=(0,0)$ is the only critical point where $h(\phi)=0$. However, wherever five grid lines of the pentagrid determined by the vectors $\mathbf{e}_i$, $i=1,\ldots,5$ come sufficiently close to meeting, $\mathbf{E}$ behaves approximately as it does at $(x,y)=(0,0)$, yielding effective defects of charge -4.

To carry out a simulation using periodic boundary conditions we substitute for the quasicrystalline patterned alignment layer a periodic approximant to a Penrose lattice which replaces three of the grid vectors $\mathbf{e}_i$, $i=3,4,5$ [Eq. (1)] by [6,7]

$$\mathbf{e}_3' = -\mathbf{e}_1 + \frac{1}{\tau_N}\mathbf{e}_2,$$

$$\mathbf{e}_4' = -\frac{1}{\tau_N}\mathbf{e}_1 - \frac{1}{\tau_N}\mathbf{e}_2,$$

$$\mathbf{e}_5' = \frac{1}{\tau_N}\mathbf{e}_1 - \mathbf{e}_2, \tag{5}$$

where $\tau_N = \frac{F_{N+1}}{F_N}$, and F_N and F_{N+1} are successive Fibonacci numbers ($F_1=1$, $F_2=2,\ldots$). As $N\to\infty$, τ_N approaches the golden ratio $\tau=(1+\sqrt{5})/2$, and the vectors $\mathbf{e}_i'$ become equal to the corresponding $\mathbf{e}_i$. For finite N the vectors $\mathbf{e}_1,\mathbf{e}_2,\mathbf{e}_3',\mathbf{e}_4',\mathbf{e}_5'$ yield a periodic pentagrid with a rhombic unit cell which has the shape of a "thick" rhombus of the corresponding Penrose tiling with sides parallel to the vectors $[\cos(\pi/10),-\sin(\pi/10)]$ and (0,1). For light with projected wave vector k, the sides of the rhombic unit cell have length L given by

$$L = \frac{2\pi F_{N+1}}{k \sin\left(\frac{2\pi}{5}\right)}. \tag{6}$$

We model a nematic liquid crystal using the Lebwohl-Lasher model [8] of rotors specified by unit vectors $\mathbf{u}_\alpha$ located at sites α of a suitably chosen lattice. Each rotor represents a small group of mesogenic molecules. The model is defined by the Hamiltonian

$$\mathcal{H} = -J\sum_{\langle\alpha\beta\rangle}\left\{\frac{3}{2}(\mathbf{u}_\alpha\cdot\mathbf{u}_\beta)^2 - \frac{1}{2}\right\}, \tag{7}$$

where the sum is over nearest neighbors on the lattice and J is a coupling parameter.

The top and bottom of our simulation box (the patterned alignment layers) are each chosen to be a single unit cell of the periodic pentagrid, i.e., a rhombus of side L. We choose the wave vector k so that L is integer valued and thus we can discretize the layers with L^2 rhombi of side unity. The two alignment layers are assumed to be identical and in registry with each other, consistent with the experimental fabrication process where the cell is assembled prior to the holographic exposure and introduction of the nematic material [3]. The remaining four sides of the box are rectangles of size $L\times H$, where H, an integer, is the height of the box. Each Lebwohl-Lasher lattice point in the box thus has position given by the vector $\mathbf{r}_\alpha = n_1[\cos(\frac{\pi}{10}),-\sin(\frac{\pi}{10}),0]+n_2(0,1,0)+n_3(0,0,1)$ where the integers n_1,n_2,n_3 satisfy $-\frac{L}{2}+1\leqslant n_1\leqslant\frac{L}{2}$, $-\frac{L}{2}+1\leqslant n_2\leqslant\frac{L}{2}$, $1\leqslant n_3\leqslant H$. The top and bottom alignment layers correspond to $n_3=1$ and H, respectively. We assume infinitely strong anchoring of the rotors on these layers, i.e., the orientation of the rotors $\mathbf{u}_\alpha$ on these layers is given by the electric field (2), with the grid vectors $\mathbf{e}_i$ replaced by their periodic counterparts.

We carried out our simulations at a temperature $T=0.1$, measured in dimensionless units of J/k_B. We initialized the system with a random configuration of rotor orientations (consistent with the experimental procedure where the nematic is introduced into the cell in the isotropic phase and then cooled) and ran simulations for 10 000 Monte Carlo cycles for thin samples ($H\lesssim 10$) and 50 000–100000 for thicker samples, where each cycle corresponds to attempted rotations of $L^2\times H$ rotors chosen at random. We implemented the attempted rotations via random displacements of ϕ_α and $\cos\theta_\alpha$, where ϕ_α and θ_α are the spherical coordinates of the rotor at site $\mathbf{r}_\alpha$. The ranges of the random displacements $\Delta\phi_\alpha$ and $\Delta\cos\theta_\alpha$ were chosen to be $-0.25<\Delta\phi_\alpha<0.25$ and $-0.025<\Delta\cos\theta_\alpha<0.025$. These choices allowed us to achieve a Monte Carlo acceptance ratio of approximately 50%. We simulated boxes of size $L=66,106,132,172$, with heights H ranging from 3 to 40. The Fibonacci numbers F_{N+1} used were $F_4=5$ for $L=66,132$; $F_5=8$ for $L=106$, and $F_6=13$ for $L=172$. Given these values the wave vector k is determined by Eq. (6).

As in the fourfold symmetric case [4], we find that nematic ordering in the simulation box and the topology of the disclination lines emerging from the defects on the patterned

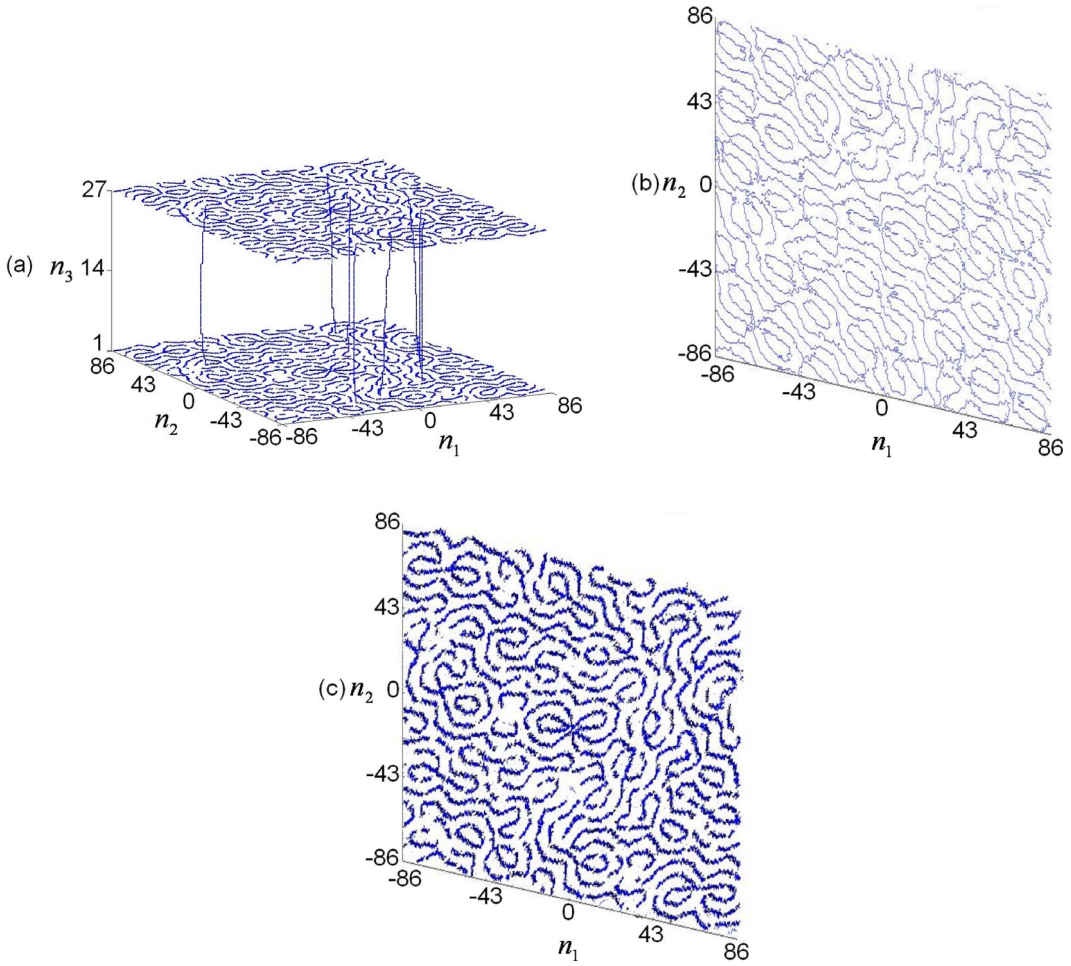

FIG. 2. (Color online) (a) Disclination lines in a simulation box of dimensions $L=172$, $H=27$. The axes are labeled by the integers n_1,n_2,n_3 which parameterize the lattice vector $\mathbf{r}_\alpha=n_1[\cos(\frac{\pi}{10}),-\sin(\frac{\pi}{10}),0]+n_2(0,1,0)+n_3(0,0,1)$. The lines that appear to lie on the top and bottom surfaces have their endpoints on these surfaces but otherwise lie one half lattice spacing into the interior of the box. (b) Curves defined by $\mathbf{E}(\mathbf{r}_\perp)\lambda=0$, which predict the disclinations for large box thicknesses such as the one shown here. In this figure λ is a function of position given by the directors of the domains for the simulation depicted in (a). (c) The $n_3=1$ layer of the pattern shown in (a), which resembles the prediction shown in (b) as expected.

surfaces depend on the thickness H of the box. In general, the system tries to minimize the length of the disclination lines. For thin enough boxes each defect in the anchoring field pattern is connected to the corresponding defect on the opposite surface by two $\pm\frac{1}{2}$ disclination lines which bifurcate from the integer-valued defect points on the surfaces (there are eight such half-integer lines emerging from the defect of charge -4 at the origin of the pentagrid). These bifurcations occur right at the boundaries. For large thicknesses, most if not all of the disclination lines hug the patterned surfaces and join point defects on a single surface. We identified the disclination lines in our simulations using the technique of Ref. [9].

In the case of fourfold symmetry it was found that the nematic order parameter vanished for small thicknesses and was nearly saturated for large thicknesses. In the latter case the nematic director was oriented parallel to the direction of the disclination lines hugging the surfaces. The local nematic director undergoes a 90° rotation as the disclination line is crossed. In this way the disclination lines mediate the change in the director orientation from the uniform order in the interior of the box to the patterned array of integer defects on the surfaces. The situation is somewhat more complicated here for the pentagrid as we find that nematic domains form in the interior of the box for large thicknesses. However, for a given domain, the physics is similar to what was found in the fourfold symmetric case. Namely, if we denote the orientation of a domain by the unit vector λ, then we find that the disclination lines are oriented generally along curves satisfying $\mathbf{E}(\mathbf{r}_\perp)\lambda=0$ (see Fig. 2). This latter condition is simply the statement that the director at the surface which is given by the electric field direction makes an angle of 90° with the director in the adjacent domain.

We found that it is possible to overlay a Penrose tiling of thick and thin rhombi of edge length $l=\frac{4\pi\tau}{5k}$ on the anchoring pattern in such a way that most $+1$ defects occur near the vertices of the tiling, and most -1 defects occur near the centers of the thick rhombi (see Fig. 1), a result consistent with the symmetries of the electric field and our estimate for the area density of defects given by our analysis of the criti-

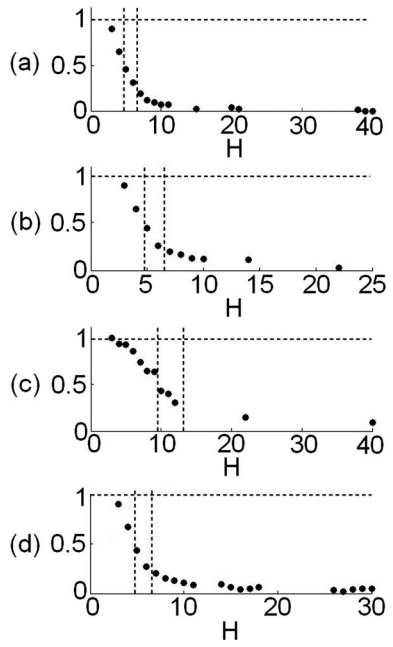

FIG. 3. Fraction of disclination lines traversing the height H of the box as a function of H for (a) $L=66$, (b) $L=106$, (c) $L=132$, and (d) $L=172$. The dashed vertical lines are drawn at $H=l_1, l_2$ [see Eq. (8)]. The dashed horizontal lines are drawn at values of the total number of disclination lines found in each case. The values of k, as determined by Eq. (6), are approximately 0.25 for $L=132$ and 0.5 for $L=66$, 106, and 172, leading to $l_1 \approx 9.6$, $l_2 \approx 13.2$ and $l_1 \approx 4.8$, $l_2 \approx 6.6$, respectively. Note that for $H=3$ nearly all of the disclination lines traverse the box, while for $H \approx l_1$ about half do, and for $H > l_2$ most of the disclinations do not traverse the box and thus hug the patterned surfaces.

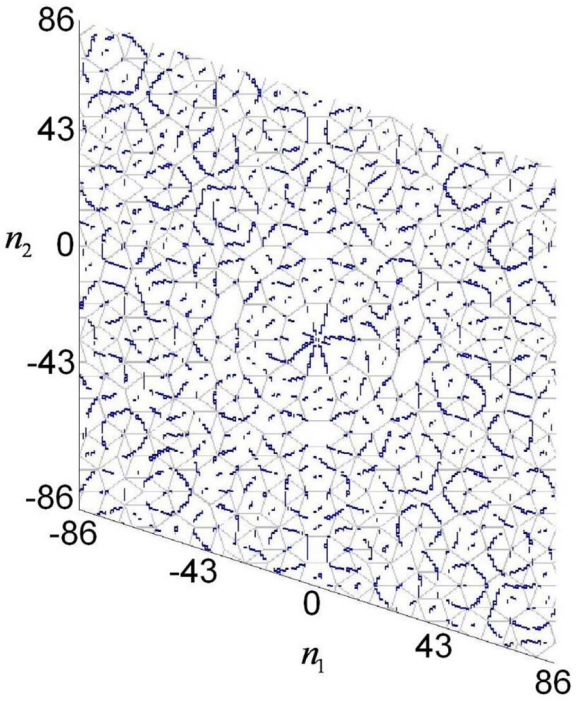

FIG. 4. (Color online) The $n_3=1$ layer of disclination lines for a simulation with $L=172$, $H=5$, with a Penrose tiling of edge length $l=\frac{4\pi\tau}{5k}$ superimposed. The set of disclination lines hugging the surface in this case is approximately the set of short diagonals of the thick rhombi of the Penrose tiling.

cal points of ϕ. The distances from the centers of such rhombi to their vertices

$$l_1 = l \sin(\pi/5), \quad l_2 = l \cos(\pi/5), \tag{8}$$

give the typical distances of -1 defects from the four nearest $+1$ defects. Given that the energy of the system prefers to minimize the length of the disclination lines, we expect that for $H \gtrsim l_2$, nearly all of the lines will hug the patterned surfaces in a formation predicted by $\mathbf{E}(\mathbf{r}_\perp)\lambda=0$, for $l_1 \lesssim H \lesssim l_2$, lines will hug the surface along most of the short diagonals of thick rhombi in the length l Penrose tiling and traverse the box elsewhere, and for $H \lesssim l_1$, most of the lines will traverse the box. Figures 3 and 4 confirm that our results agree with these expectations.

In summary, we carried out simulations of the Lebwohl-Lasher model of a nematic liquid crystal confined to a cell with two opposing surfaces patterned with an anchoring field with fivefold quasicrystalline symmetry. The patterning introduces point topological defects which primarily have charge ± 1. Half-integer disclination lines emerge from these defects and either traverse the cell for large cell thicknesses, hug the patterned surfaces for small thicknesses, or combine these behaviors for intermediate thicknesses. An estimate of the critical thicknesses can be obtained using the properties of Penrose tilings.

We are grateful to G. P. Crawford and S. P. Gorkhali for very helpful discussions which motivated our work.

[1] W. M. Gibbons, P. J. Shannon, S. T. Sun, and B. J. Swetlin, Nature (London) **351**, 49 (1991).
[2] B. W. Lee and N. A. Clark, Science **291**, 2576 (2001).
[3] G. P. Crawford, J. N. Eakin, M. D. Radcliffe, A. Callan-Jones, and R. A. Pelcovits, J. Appl. Phys. **98**, 123102 (2005).
[4] A. S. Backer, A. C. Callan-Jones, and R. A. Pelcovits, Phys. Rev. E **77**, 021701 (2008).
[5] N. G. Debruijn, Math. Program. Ser. A **84**, 39 (1981).
[6] H. Tsunetsugu, T. Fujiwara, K. Ueda, and T. Tokihiro, Phys. Rev. B **43**, 8879 (1991).
[7] O. Entin-Wohlman, M. Kleman, and A. Pavlovitch, J. Phys. (Paris) **49**, 587 (1988).
[8] P. A. Lebwohl and G. Lasher, Phys. Rev. A **6**, 426 (1972).
[9] M. Zapotocky, P. M. Goldbart, and N. Goldenfeld, Phys. Rev. E **51**, 1216 (1995).